Available online at www.sciencedirect.com
SCIENCE DIRECT
International Journal of Heat and Mass Transfer 49 (2006) 2965–2971
International Journal of HEAT and MASS TRANSFER
www.elsevier.com/locate/ijhmt

Heat transfer enhancement of transverse ribs in circular tubes with consideration of entrance effect

Jung-Yang San *, Wen-Chieh Huang

Department of Mechanical Engineering, National Chung Hsing University, 250, Kao-Kuang Road, Taichung 40227, Taiwan, ROC

Received 28 October 2004; received in revised form 10 January 2006
Available online 17 April 2006

Abstract

The heat transfer enhancement of transverse ribs in circular tubes with a length-to-diameter ratio of 87 was experimentally investigated. The mean heat transfer and friction data were obtained for the air flow started from the entrance. An isothermal surface condition was considered. The rib pitch-to-tube diameter ratio (p/d) was in the range 0.304–5.72; the rib height-to-tube diameter ratio (e/d) was in the range 0.015–0.143; the considered Reynolds number (Re) was in the range 4608–12,936. The mean Nusselt number (Nu) and friction factor (f) were individually correlated as a function of p/d, e/d and Re. A critical e/d, equal to 0.057, was found. For $e/d < 0.057$, the f is proportional to e/d; for $e/d \geqslant 0.057$, the f is proportional to $(e/d)^{2.55}$. A performance map, indicating the corresponding heat transfer enhancement index (r_1) and efficiency index (r_2) for various p/d and e/d, was constructed. This performance map clearly indicates the ranges of p/d and e/d with a high r_2.

Keywords: Heat transfer enhancement; Transverse ribs; Efficiency index; Performance map

1. Introduction

In the past few decades, tremendous researches had been performed on heat transfer enhancement in tubes. The goals of these researches aimed at finding techniques not only increasing heat transfer, but also achieving high efficiency. Comprehensive assessments of these techniques are available in the literature [1–3].

Webb et al. [4] investigated the heat transfer and fluid friction for fully developed turbulent flow in tubes with transverse ribs. The tubes were arranged with a constant surface heat flux condition. A set of correlations of Stanton number and friction factor was obtained. The flow field in a parallel-plate channel with staggered ribs was numerically analyzed by Webb and Ramadhyani [5]. The result shows that, for a large rib height-to-channel spacing ratio, the flows in the separated zones (before and after the ribs) significantly affect the main flow. This results in a substantially high friction factor for the flow. The heat transfer in a circular tube with a slat-like blockage was investigated by Sparrow et al. [6]. The heat transfer enhancement was found to be effective within a distance of 10 tube diameters downstream of the blockage. Gee and Webb [7] reported a study of the heat transfer in circular tubes with helical ribs. The result shows that the tube with rib helical angle of 49° provides the highest heat transfer rate per unit pumping power. Sethumadhavan and Raja Rao [8] reported an optimization study of helical-wire-core inserts in circular tubes. The result indicates that, for different fluids, the optimum rib helical angle would slightly vary. Uttarwar and Raja Rao [9] also investigated the heat transfer enhancement of helical-wire-core inserts in circular tubes. The result shows that the augmentation of heat transfer for low Reynolds number operations is much more pronounced than that for high Reynolds number operations. Royal and Bergles [10] compared the condensation augmentation in tubes

* Corresponding author. Tel.: +011 886 04 2840433x318; fax: +011 886 04 2851941.
E-mail address: jysan@dragon.nchu.edu.tw (J.-Y. San).

0017-9310/$ - see front matter © 2006 Elsevier Ltd. All rights reserved.
doi:10.1016/j.ijheatmasstransfer.2006.01.046

Nomenclature

c_p	specific heat, J/kg K	T	temperature, °C
d	tube inside diameter (at base of ribs), m	u	mean fluid velocity, m/s
e	rib height (roughness), m		
f	Darcy friction factor	*Greek symbols*	
h	convective heat transfer coefficient, W/m^2 K	ρ	air density
k	thermal conductivity, W/m K	μ	dynamic viscosity, kg/m s
L	tube length, m		
$\dot{m}$	air mass flowrate, kg/s	*Subscripts*	
Nu	Nusselt number, hd/k	1–4	measuring points
p	rib pitch, m	a	air
P	pressure, Pa	i	inlet
ΔP	pressure drop, Pa	o	smooth tube or outlet
r_1	heat transfer enhancement index, Nu/Nu_0	s	tube surface
r_2	efficiency index, $(Nu/Nu_0)/(f/f_0)$	w	water
Re	Reynolds number, $\rho ud/\mu$ or $4\dot{m}/\pi d\mu$		

with twisted-tape inserts to that with internal fins. It was found that the latter is much higher than the former. Goto et al. [11,12] investigated the condensation and evaporation augmentations in internally grooved tube. The measured data yield a set of Nusselt number correlations. Fernadez and Poulter [13] proposed a flag-type insert for heat transfer enhancement in circular tubes. The measured data reveal that, with the insert, the increase in pressure drop is less than that in heat transfer. Wang et al. [14] investigated the heat transfer in a channel with metallic-filament inserts. The result shows that, for low Reynolds number operations, the inserts are quite effective to enhance the heat transfer.

Most of the previously measured data, relating to heat transfer enhancement in tubes, were obtained based on the flow completely in the fully developed region. Undoubtedly, these data are quite useful in designing large-size heat exchangers which are composed of long tubes. However, directly using these data in designing small-size heat exchangers, without considering the entrance effect, inevitably it would result in an uncertainty. In this work, the heat transfer enhancement of transverse ribs in circular tubes (Fig. 1) with a length-to-diameter ratio (L/d) of 87 was experimentally investigated. Based on the measured data, it is intended to find the best ranges of rib height-to-tube diameter ratio (e/d) and rib pitch-to-tube diameter ratio (p/d) for efficient heat transfer enhancement.

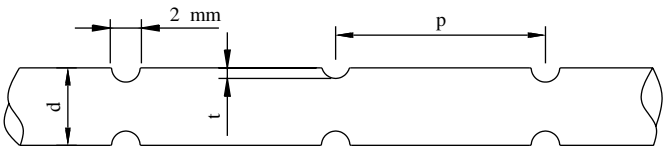

Fig. 1. A tube with internal transverse ribs.

2. Apparatus and experimental procedure

Fig. 2 shows the schematic of the measuring system. A one-horsepower air blower was used in the experiment. The air flowrate of the blower was adjusted for various Reynolds numbers by controlling the frequency of the electricity with an electric converter. A rotameter with a maximum error of 5% was installed at the outlet of the system to monitor the air volumetric flowrate. A surge tank with volume of 0.3 m^3 was connected in the air supply line to reduce the pressure fluctuation of the air. In this work, one smooth copper tube and nine rib-roughened copper tubes were individually tested. The length of the tubes was 1.2 m. The wall thickness of the tubes was 1 mm and the inside diameter (at the base of the ribs) was 13.8 mm. The corresponding e/d and p/d of the nine rib-roughened tubes are specified in Table 1.

For every test, a specific tube was installed and well-sealed in a tank filled with water. The water was heated using two electric heaters. One was rated at 2000 W and the other was 1000 W. The water temperature in the tank was controlled by a PID controller. A one-horsepower pump was used to circulate the water in the tank. The

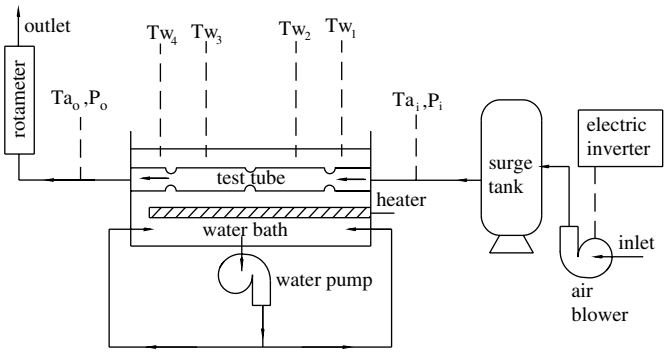

Fig. 2. Schematic of measuring system.

Table 1
r_1 and r_2 for $Re = 10{,}633$

Tubes	Specifications	r_1	r_2
1	$p/d = 5.72$, $e/d = 0.075$	1.50	0.67
2	$p/d = 5.0$, $e/d = 0.05$	1.33	0.90
3	$p/d = 4.29$, $e/d = 0.075$	1.65	0.55
4	$p/d = 2.86$, $e/d = 0.057$	1.54	0.62
5	$p/d = 1.43$, $e/d = 0.143$	2.46	0.07
6	$p/d = 1.43$, $e/d = 0.057$	1.73	0.56
7	$p/d = 0.75$, $e/d = 0.015$	1.21	0.97
8	$p/d = 0.5$, $e/d = 0.0643$	2.10	0.32
9	$p/d = 0.304$, $e/d = 0.0286$	1.67	0.59

water flow was regulated to flow fast enough to achieve a large convection effect on the external surface of the tube. This would insure a uniform temperature distribution on the tube surface. The water temperature was carefully examined using four T-type thermocouples which were located along the outer surface of the tube. The maximum temperature deviation among the four thermocouples was determined to be 0.2 °C. The air temperatures at the inlet and outlet of the test tube were individually measured using two shielded T-type thermocouples. All the signals from the thermocouples were processed by the Hp-3856 data-acquisition system. A U-tube manometer was used to measure the pressure drop of the air between the inlet and outlet of the test tube. The ratio of free flow area to frontal area at the inlet and outlet was 0.77.

In this work, an isothermal surface condition was arranged for the test tubes. The mean Nusselt numbers for the air inside the tubes can be individually obtained by substituting the corresponding inlet and outlet air temperatures into the following equation [15]:

$$Nu = -\left(\frac{d}{k}\right)\left(\frac{\dot{m}c_p}{\pi dL}\right)\ln\left[\frac{T_s - T_o}{T_s - T_i}\right] \quad (1)$$

The Darcy friction factors for the test tubes operating at various Reynolds numbers were individually obtained by substituting the corresponding pressure drops directly into the following equation [15]:

$$f = \frac{\Delta P}{(L/d)[\rho u^2/2]} \quad (2)$$

In the above equation, u stands for the mean air velocity which is equal to the air volumetric flowrate divided by the cross-sectional area of the flow passage in the region without the ribs.

3. Results of measurement

Fig. 3 represents the measured Nu of the test tubes. The result shows that, for each tube, the Nu almost linearly increases with the Re. In the diagram, the solid line ($e/d = 0$) represents the present measured result for the smooth tube and the dotted line indicates the corresponding correlation result provided by Gnielinski [16]. The result indicates that the former is about 10% lower than the latter.

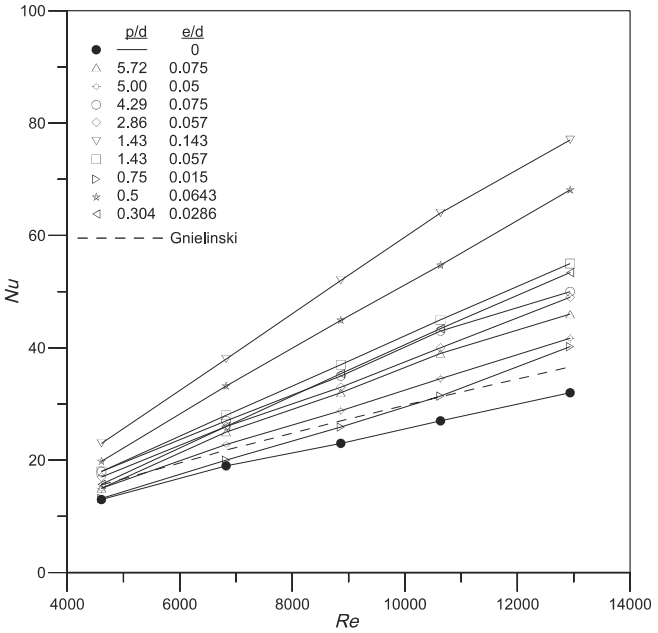

Fig. 3. Nu for various p/d, e/d and Re.

Fig. 4 represents the measured friction coefficients of the 10 test tubes. As indicated, for the tube with $e/d = 0.143$ and $p/d = 1.43$, the f exceeds 1.0 which is 20 times larger than that of the smooth tube; for the tube with $e/d = 0.057$ and $p/d = 1.43$, the f is only 0.13. This implies that the e/d is the key factor dominating the magnitude of the f.

Fig. 4 shows that, for a change of the Re, the variation of f of the rib-roughened tubes is much smaller than that of the smooth tube. It also shows that, for every test tube except the smooth tube and the tube with the e/d of

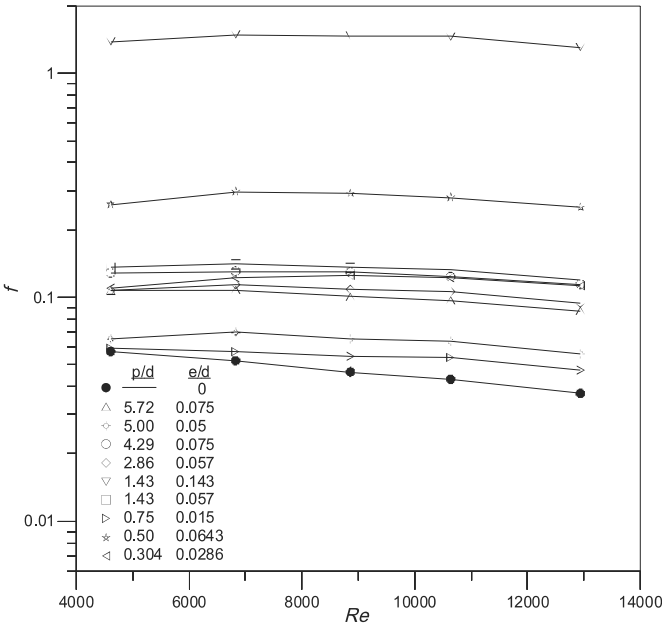

Fig. 4. f for various p/d, e/d and Re.

0.015, correspondingly there is a maximum f occurring at a specific Re in the range 6000–9000. This implies that, to the left of the maximum (low Re operations), the flow disturbance induced by the ribs is relatively weak. For the tube with the e/d of 0.015, its rib height (e) is much smaller than those of the other tubes. The variation of f of this tube tends to be closer to that of a smooth tube and there is no maximum f appearing in the considered range of Re.

For the smooth tube, at a specific Re, the present measured f is larger than the corresponding f showing in the Moody diagram [15]. In this work, the effect of entry length and the effects of contraction and expansion at the inlet and outlet of the tube were considered in the measurement. But the f showing in the Moody diagram only represents the data in the fully developed region. Thus for the operation with $Re = 4608$, there is a deviation of 43% between our measured result and the data showing in the Moody diagram; for the operation with $Re = 12{,}936$, the deviation is 28%. This deviation decreases with an increase of the Re.

As shown in Fig. 4, for the rib-roughened tubes, the f only slightly varies with the Re. However, for the smooth tube, its f (f_0) substantially decreases with an increase of the Re. Thus the ratio, f/f_0, tends to increase with the Re.

The measured Nu and f can be used to evaluate the corresponding r_1 and r_2 of each test tube. Table 1 shows the r_1 and r_2 of the nine rib-roughened tubes for the Re of 10,633. As indicated, tube (5) possesses the highest value of r_1, but its corresponding value of r_2 is the lowest; conversely, tube (7) has the highest value of r_2, but its r_1 is the lowest. The value of r_2 for tube (7) is 0.97. This means that, for this specific tube, the increase in h is about the same as the increase in f. Hence, the operation with this tube is quite efficient in terms of heat transfer rate per unit pumping power. The value of r_2 for tube (5) is only 0.07. From the energy-saving viewpoint, the operation with this tube is quite inefficient. Among all the test tubes, tube (5) possesses the largest value of e/d, but its r_2 is much lower than those of the others. This implies that, in designing rib-roughened tubes for efficient operations, the e/d should be limited within a certain range.

Fig. 5 shows the r_2 of the nine rib-roughened tubes in operations with various Reynolds numbers. The result indicates that, except at $Re = 4608$, for each test tube the values of r_2 are quite uniform in the considered range of Re. The results shown in Fig. 5 and Table 1 are helpful to realize the effects of e/d and p/d on the r_1 and r_2. However, similar to those data in the literature, it only provides piecewise information of the r_1 and r_2. A comprehensive understanding of the heat transfer and friction characteristics of the rib-roughened tubes cannot be achieved merely by analyzing these limited data.

4. Correlations

Fig. 6 shows the correlation of the Nu. As indicated, all the measured heat transfer data can be correlated using a simple equation as follows:

$$Nu = 0.0072(Re)^{1.05}(p/d)^{-0.15}(e/d)^{0.333} \quad (3)$$

In the above equation, the fluid properties should be evaluated at the mean fluid temperature. An error analysis was performed for the above heat transfer correlation. The result shows that the mean error between the correlation result and measured data is 4.7%; the maximum error is 17.4% which occurs at the Re of 4608. In this work, a measured Nu obtained by Webb et al. [4] was plotted in Fig. 6 to compare with the current correlation result. As indicated, their data is 15% greater than the current predicted

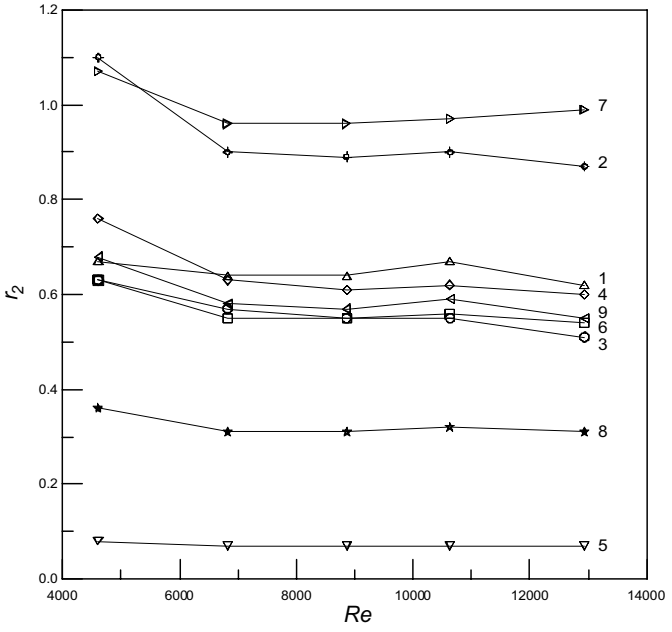

Fig. 5. Effect of Re on r_2.

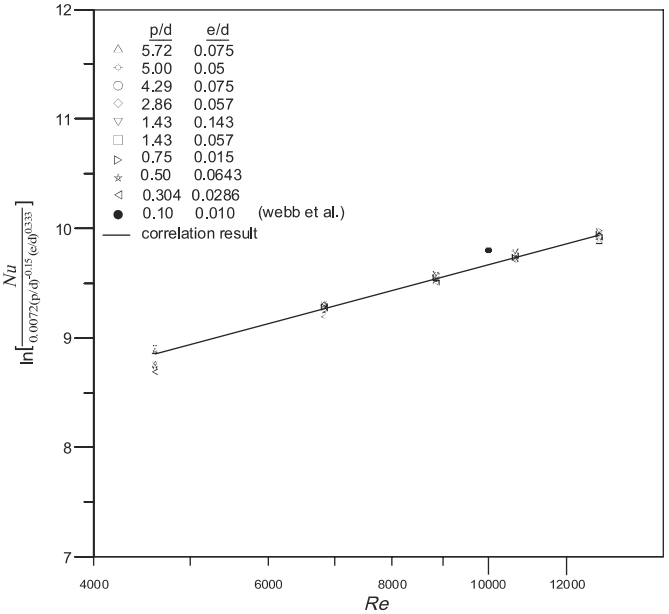

Fig. 6. Correlation of Nu.

result. In their work, the measurement was based on a constant surface heat flux condition. In this work, the test tubes were arranged with a constant surface temperature condition. This could be the main reason resulting in the deviation. It is worth to mention that the *Nu* provided by Webb et al. [4] corresponds to a tube with $p/d = 0.1$ and $e/d = 0.01$. Both these two values are beyond the present considered range. Furthermore, the ribs in their tube were with a sharp edge, instead of a smooth edge as those in our tubes. Besides that, in their experiment only fully developed flow was considered, but in our experiment both entrance flow and fully developed flow were included. Despite having all these differences, the result shows that Eq. (3) can be applied to predict their data with an acceptable accuracy. This implies that the thermal entry length of the rib-roughened tubes is quite short. Thus the effect of entrance region on the heat transfer is insignificant.

As shown in Eq. (3), the *Nu* is proportional to $(e/d)^{0.333}$ and it is inversely proportional to $(p/d)^{0.15}$. This indicates that the effect of e/d on the *Nu* is stronger than that of p/d. Eq. (3) also shows that the *Nu* is proportional to $Re^{1.05}$. As indicated in the Dittus–Boelter equation [15], for turbulent flow in a smooth circular tube, the *Nu* is proportional to $Re^{0.8}$. This implies that the effect of *Re* on the *Nu* for the rib-roughened tubes is stronger than that for a smooth tube. It results that the r_1 would slightly increase with the *Re*.

Fig. 7 represents the correlation of the measured f. As shown in the result, for the e/d greater than 0.057, the increasing rate of f would largely increase. This could be due to a significant increase of the flow recirculation before and after the ribs. This flow recirculation would form a blockage in the flow passage and significantly affect the main flow. This phenomenon also had been pointed out by Webb and Ramadhyani [5]. Thus the present result shows that the increasing rate of f for $e/d > 0.057$ is much greater than that for $e/d < 0.057$. Based on the result as shown in Fig. 7, the measured data of f were correlated into the following equations:

$$f = 0.0018(e/d)\mathrm{e}^{-0.26(p/d)}(Re)\mathrm{e}^{-1.44\times10^{-4}Re} \quad \text{for } 0.015 \leqslant e/d < 0.057 \tag{4}$$

$$f = 0.132(e/d)^{2.55}\mathrm{e}^{-0.26(p/d)}(Re)\mathrm{e}^{-1.44\times10^{-4}Re} \quad \text{for } 0.057 \leqslant e/d \leqslant 0.143 \tag{5}$$

where the fluid properties should be evaluated at the mean fluid temperature. Using the above two equations to correlate the measured data, it yields a mean error of 8.7% and a maximum error of 15.5%. In this work, a more accurate correlation for the e/d in the range 0.015–0.05 was used in plotting a performance map for the rib-roughened tubes. This correlation is expressed as follows:

$$f = 0.0023(e/d)^{1.04}\mathrm{e}^{-0.26(p/d)}(Re)\mathrm{e}^{-1.44\times10^{-4}Re} \quad \text{for } 0.015 \leqslant e/d \leqslant 0.05 \tag{6}$$

Most existing heat transfer correlations for circular tubes with transverse ribs express Nusselt number as a function of f and other related parameters. Webb et al. [4] had proposed a correlation of this type. In this work, a comparison of their correlation with ours, for the test tube with $e/d = 0.0286$ and $p/d = 0.304$ operating at the Reynolds number of 10,633, was performed. Substituting our measured value of f into their correlation equation, a predicted Nusselt number of 62.2 was obtained. Using our correlation, it yields a predicted value of 44.6. For the same tube and operating condition, our measured data shows that the Nusselt number is 44.6. As clearly indicated, our predicted value is quite close to the measured data, but their predicted value is largely over-estimated. The main reason to cause this significant discrepancy is attributed to a deviation in the measuring conditions. In our experiment, the measurement of f considers not only the pressure drop across the tube, but also the contraction and expansion effects at the entrance and exit. In their experiment, the measurement of f was only conducted in the fully developed region. This results that the obtained value of f from our measurement is larger than that from theirs. Hence, substituting our measured value of f into their heat transfer correlation inevitably results in an over-estimation of the Nusselt number. This also implies that their correlation is not applicable to our considered cases.

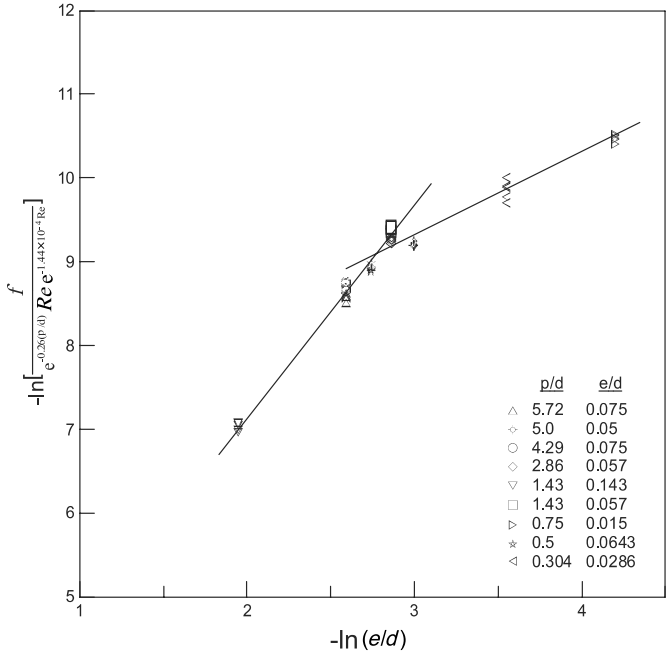

Fig. 7. Correlation of f.

5. Performance map

Fig. 8 shows the performance map of the rib-roughened tubes for the *Re* of 10,633. This diagram was plotted based on the correlation results as shown in the above. For a tube with a set of r_1 and r_2, the corresponding e/d and p/d can be

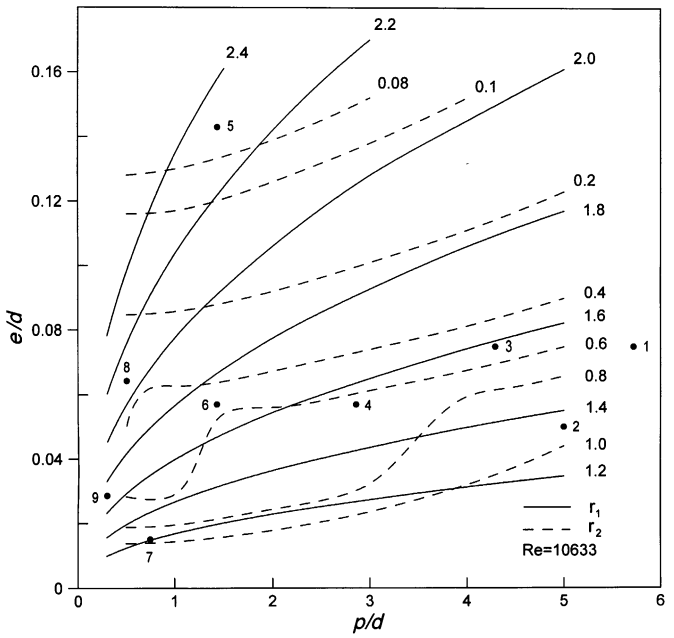

Fig. 8. Performance map for $Re = 10{,}633$.

directly found from Fig. 8. Besides that, Fig. 8 also shows a clear picture of the effects of e/d and p/d on the r_1 and r_2. As indicated in the diagram, for a specific p/d, the r_1 would increase with the e/d. Similarly, for a specific e/d, the r_1 would increase with a decrease of the p/d. The result also shows that the effect of e/d on the r_1 is stronger than that of p/d. The effects of e/d and p/d on the r_2 are completely reversed to those on the r_1. For a specific p/d, the r_2 would increase with a decrease of the e/d. For a specific e/d, the r_2 would increase with the p/d.

As shown in the earlier, for the e/d greater than 0.057, the f is proportional to $(e/d)^{2.55}$; for the e/d less than 0.057, the f is proportional to e/d. This results that the effect of e/d on the f for $e/d < 0.057$ is much less than that for $e/d > 0.057$. Thus in Fig. 8, the constant r_2 curves in the region $e/d < 0.057$ appear to be quite different from those in the region $e/d > 0.057$. In the region $e/d > 0.057$, for an increase of the e/d on a constant r_2 curve, the r_1 would initially decrease and then it would remain almost the same; but in the region $e/d < 0.057$, in a certain range of the p/d, the r_1 would increase.

In Fig. 8, for the r_2 in the range 0.4–0.8, on each constant r_2 curve, there is a region showing an abrupt rise of the e/d for a small increase of the p/d. It indicates that there exists a critical point on each constant r_2 curve. To the left of the critical point (in the region with a small p/d), for a decrease of the p/d, the r_1 would increase, but the corresponding e/d does not vary much. This increase in heat transfer is attributed to an increase of the heat transfer area and an increase of the flow disturbance. Both result from a decrease of the rib pitch. To the right of the critical point (in the region with a large p/d), for a small increase of the p/d, the e/d would apparently increase. Correspondingly, the r_1 would also increase. This increase in heat transfer is simply due to an increase of the flow disturbance resulting from an increase of the rib height.

Most of the previous works [4,7] investigated the heat transfer characteristics for tubes with small p/d ($\leqslant 0.8$) and e/d ($\leqslant 0.04$). As indicated in Fig. 8, for $p/d \leqslant 0.75$ and $0.01 \leqslant e/d \leqslant 0.02$, the r_2 can be greater than 0.8 and r_1 can be greater than 1.3. Thus the region with small p/d and e/d indeed provides a high r_2 and a relatively high r_1. In this work, another region with a large p/d ($\geqslant 3.0$) and a relatively large e/d (0.03–0.057) was also found to possess a high r_2 and a relatively high r_1. As pointed out by Sparrow et al. [6], the heat transfer enhancement of a slat-like blockage in a circular tube is effective within a distance of 10 tube diameters downstream of the blockage. Physically, the blockage in their tube is quite similar to a single transverse rib in our tubes. Thus for a specific rib height (e), a certain amount of the ribs in a tube would be enough to achieve a continuation of the flow disturbance, thereby inducing an effective heat transfer enhancement. At this situation, a further increase of the ribs would cause a substantial increase of the pressure drop, but the increase in heat transfer would be quite limited. This is the reason why the region with a large p/d ($\geqslant 3.0$) and a relatively large e/d (0.03–0.057) also possesses a high r_2 (>0.8) and a relatively high r_1 (>1.3).

In Fig. 8, Pts. 1–9 individually represent the corresponding positions of the nine test tubes on the performance map. The corresponding r_1 and r_2 of the nine points in Fig. 8 are slightly different from those in Table 1. The individual deviation is less than 10%.

6. Conclusions

In this work, the measured data of Nu for the flow in the rib-roughened tubes were successfully correlated into a simple equation. It was found that the effect of entrance region on the Nu is small. The effect of e/d on the Nu appears to be stronger than that of p/d. As indicated in the result, the Nu is proportional to $(e/d)^{0.333}$ and it is inversely proportional to $(p/d)^{0.15}$. The result also shows that the Nu almost linearly increases with the Re.

For the rib-roughened tubes, the influence of Re on the f is quite weak. The f only slightly varies with the Re. A critical e/d, equal to 0.057, was found. For the e/d greater than 0.057, the f is proportional to $(e/d)^{2.55}$; for the e/d less than 0.057, the f is directly proportional to the e/d. This implies that, for efficient operations, the e/d should be less than 0.057.

As indicated in the performance map, for a specific p/d, the r_1 would increase with the e/d, but the r_2 would increase with a decrease of the e/d. Conversely, for a specific e/d, the r_1 would increase with a decrease of the p/d, but the r_2 would increase with the p/d. The measured data also shows that the r_2 only slightly varies with the Re.

The performance map not only provides the corresponding values of r_1 and r_2 for a specific rib-roughened tube, but also shows a clear picture of the ranges of p/d

and e/d with a high r_2. As indicated in the performance map, there are two regions providing a high r_2 and a relatively high r_1. One is in the region with a small p/d and a small e/d; the other is in the region with a large p/d and a relatively large e/d. Based on the performance map, in order to achieve the r_2 greater than 0.8 and r_1 greater than 1.3, the p/d should be either less than 0.75 or greater than 3.0. For the former, the corresponding e/d should be in the range 0.01–0.02; for the latter, the corresponding e/d should be in the range 0.03–0.057.

References

[1] A.E. Bergles, Principles of Heat Transfer Augmentation, Heat Exchangers, Thermal-Hydraulic Fundamentals and Design, Hemisphere, New York, 1981, pp. 819–842.
[2] A.E. Bergles, Heat exchanger, in: G.F. Hewitt (Ed.), Heat Exchanger Design Handbook—Part 1, Begell House, New York, 1998 (Chapter 2).
[3] R.L. Webb, in: S. Kakac, R.K. Shah, W. Aung (Eds.), Handbook of Single-Phase Convective Heat Transfer, Wiley-Interscience, New York, 1987 (Chapter 17).
[4] R.L. Webb, E.R.G. Eckert, R.J. Goldstein, Heat transfer and friction in tubes with repeated-rib roughness, Int. J. Heat Mass Transfer 14 (1971) 601–617.
[5] B.W. Webb, S. Ramadhyani, Conjugate heat transfer in a channel with staggered ribs, Int. J. Heat Mass Transfer 28 (1985) 1679–1687.
[6] E.M. Sparrow, K.K. Koram, M. Charmchi, Heat transfer and pressure drop characteristics induced by a slat blockage in a circular tube, ASME J. Heat Transfer 102 (1980) 64–70.
[7] D.L. Gee, R.L. Webb, Forced convection heat transfer in helically rib-roughened tubes, Int. J. Heat Mass Transfer 23 (1980) 1127–1136.
[8] R. Sethumadhavan, M. Raja Rao, Turbulent flow heat transfer and fluid friction in helical-wire-coil-inserted tubes, Int. J. Heat Mass Transfer 26 (1983) 1833–1845.
[9] S.B. Uttarwar, M. Raja Rao, Augmentation of laminar flow heat transfer in tubes by means of wire coil inserts, ASME J. Heat Transfer 107 (1985) 930–935.
[10] J.H. Royal, A.E. Bergles, Augmentation of horizontal in-tube condensation by means of twisted-tape inserts and internally finned tubes, ASME J. Heat Transfer 100 (1978) 17–24.
[11] M. Goto, N. Inoue, N. Ishiwatari, Condensation and evaporation heat transfer of R410A inside internally grooved horizontal tubes, Int. J. Refrig. 24 (2001) 628–638.
[12] M. Goto, N. Inoue, R. Yonemoto, Condensation heat transfer of R410A inside internally grooved horizontal tubes, Int. J. Refrig. 26 (2003) 410–416.
[13] J.L. Fernandez, R. Poulter, Heat transfer enhancement by means of flag-type insert in tubes, Int. J. Heat Mass Transfer 30 (1987) 2603–2609.
[14] S. Wang, Z.Y. Guo, Z.X. Li, Heat transfer enhancement by using metallic filament insert in channel flow, Int. J. Heat Mass Transfer 44 (2001) 1373–1378.
[15] F.P. Incropera, D.P. De Witt, Fundamentals of Heat and Mass Transfer, fourth ed., Wiley, New York, 1996, pp. 424–436.
[16] V. Gnielinski, New equations for heat and mass transfer in turbulent pipe and channel flow, Int. Chem. Eng. 16 (1976) 359–368.